



Effects of ocean acidification on toxicity of two trace metals in two marine molluscs in their early life stages

Xiaoyu Guo^{1,2,4}, Miaoqin Huang^{3,4}, Bo Shi^{3,4}, Weiwei You^{3,4,5}, Caihuan Ke^{3,4,5,*}

¹College of Oceanology and Food Science, Quanzhou Normal University, Quanzhou 362000, PR China

²Fujian Province Key Laboratory for the Development of Bioactive Material from Marine Algae, Quanzhou Normal University, Quanzhou 362000, PR China

³State Key Laboratory of Marine Environmental Sciences, Xiamen University, Xiamen 361102, PR China

⁴College of Ocean and Earth Sciences, Xiamen University, Xiamen 361102, PR China

⁵State-Province Joint Engineering Laboratory of Marine Bioproducts and Technology, Xiamen University, Xiamen 361102, PR China

ABSTRACT: Ocean acidification (OA) is usually thought to change the speciation of trace metals and increase the concentration of free metal ions, hence elevating metal bioavailability. In this study, embryos of the oyster *Crassostrea angulata* and abalone *Haliotis discus hannai* were cultured under 4 pCO₂ conditions (400, 800, 1500 and 2000 µatm) with Cu and Zn added. Fertilization rate was measured 2 h post-fertilization (hpf), while larval deformation and larval shell length were measured 24 hpf. Our results show that OA can alleviate Cu and Zn inhibition of *C. angulata* fertilization by 86.1 and 26.4 % respectively, and Zn inhibition of *H. discus hannai* fertilization by 43.7%. However, OA enhanced the inhibitory effect of Cu on fertilization of *H. discus hannai* by 34.7%. OA enhanced the toxic effect of Cu on larval normality of *C. angulata* by 22.0% and the effect of Cu and Zn on larval normality of *H. discus hannai* by 71.4 and 37.2%, respectively. OA also enhanced the inhibitory effects of Cu and Zn on larval calcification in *H. discus hannai* by 8.8 and 8.6%, respectively. However, OA did not change the effect of Cu on the calcification of *C. angulata* larvae. OA decreased Zn inhibition of oyster larval calcification from 3.1 to 1.5%. Based on our results, the toxic effects of metal on early development of molluscs are not always increased by rising pCO₂ and differ across developmental stages, egg structure and species. This complexity suggests that caution should be taken when carrying out multiple environmental stressor tests on molluscan embryos.

KEY WORDS: Oyster · Abalone · Ocean acidification · Trace metal · Fertilization · Larvae

1. INTRODUCTION

Carbon dioxide (CO₂) discharged by anthropogenic activities has caused a sharp increase in atmospheric CO₂. In 2004, atmospheric pCO₂ had risen from the preindustrial concentration of 280 µatm to 380 µatm (Sabine et al. 2004); by 2017 it had risen to 405.0 µatm (Lindsey 2020). Approximately one third of anthropogenic CO₂ is absorbed by the ocean,

thereby causing reduced pH and calcium carbonate saturation, and it is predicted that 69 % of the surface ocean will acidify by more than 0.2 pH units relative to preindustrial levels by the end of the 21st century (Gattuso et al. 2015). In addition, in coastal seawater, eutrophication due to anthropogenic activities could promote the production of algae, whose decomposition and remineralization would release large amounts of CO₂, leading to the acidification of subsurface sea-

*Corresponding author: chke@xmu.edu.cn

© The authors 2020. Open Access under Creative Commons by Attribution Licence. Use, distribution and reproduction are unrestricted. Authors and original publication must be credited.

water. Therefore, coastal water which receives massive terrestrial input may be affected by both ocean acidification (OA) and local acidification, and is predicted to suffer further pH reduction compared with offshore seawater in the future (Cai et al. 2011). In a marginal sea of China (Yellow Sea), seasonal acidification has been observed in bottom seawater with a pH value of 7.90 (pH is expressed in total scale) and is predicted to further reduce to a pH of 7.80–7.85 by 2050 (Zhai 2018).

Increased $p\text{CO}_2$ can directly affect physiological functions controlling gas exchange in marine organisms. Elevated ambient CO_2 could reduce the $p\text{CO}_2$ gradient from aquatic animals to their environment, hence inhibiting CO_2 excretion and causing hypercapnia which leads to acidosis (Heuer & Grosell 2014). In addition, decreased calcium carbonate saturation may hinder calcification of marine organisms, resulting in thinner and smaller shells, making them more vulnerable to predators (Gazeau et al. 2013). The effects of OA on embryos and larvae of calcareous marine organisms have been extensively reviewed (Byrne 2010, 2011, 2012, Dupont et al. 2010, Kroeker et al. 2013). There is compelling evidence that OA can adversely affect early life stages of these organisms, with biological effects including reduced fertilization, hatching, growth and calcification, and increased larval deformation.

In addition to OA, trace metals are another environmental threat, and toxicity of trace metals to marine molluscan embryos and larvae has been studied in oysters *Crassostrea virginica* (Calabrese et al. 1977), mussels *Mytilus edulis* (Johnson 1988) and abalone *Haliotis rubra* (Gorski & Nuggeoda 2006). Toxicity of trace metals occurs through non-specific binding with enzymes and transcription factors or through metal-induced oxidative damage to proteins and critical cellular components (Stohs & Bagchi 1995, Ringwood et al. 1998, Geret et al. 2002, Dailianis et al. 2005, Valko et al. 2005, Martelli et al. 2006). Coastal regions may be affected by both OA and trace metal pollution from various sources, including wastewater discharge, antifouling paints and coastal engineering. After decades of rapid industrial expansion and ineffective pollution management, trace metal contamination has frequently been observed in coastal environments in China (Pan & Wang 2012).

OA likely changes the speciation of metals by increasing concentrations of free ions such as Cu and Zn (Millero et al. 2009), thereby increasing bioavailability of trace metals and aggravating their toxicity in estuaries. The combined effects of OA and trace metals have been studied in polychaetes (Lewis et al.

2013), molluscs (Lacoue-Labarthe et al. 2009, Ivanina et al. 2013, Götze et al. 2014, Belivermiş et al. 2016, Shi et al. 2016) and copepods (Pascal et al. 2010, Fitzer et al. 2013, Li et al. 2017). In contrast to predictions that OA would increase the toxicity of some trace metals (Millero et al. 2009), the results of these studies showed complex responses of marine organisms to the combined influence of OA and trace metals. For example, fertilization of the polychaete *Pomatosceros lamarckii* was unaffected by adding Cu to ambient or acidified seawater, while larval survival significantly decreased when Cu and OA co-occurred relative to OA only (Lewis et al. 2013). OA enhanced Cu and Cd accumulation in mantle tissue of oysters *C. virginica* and hard clams *Mercenaria mercenaria*, and proteasome responses to metals in those species were also modulated by OA (Götze et al. 2014). Cd accumulation in 3 bivalve species (*Mytilus edulis*, *Tegillarca granosa* and *Meretrix meretrix*) was significantly higher in CO_2 -acidified seawater (Shi et al. 2016). Greater decline in copepod naupliar production was observed in seawater with decreasing pH when Cu was added than in seawater with decreasing pH alone; however, Cu addition enhanced copepod growth regardless of pH level (Fitzer et al. 2013). OA could even alleviate the toxic effects of Hg on copepod reproduction by reducing its accumulation (Li et al. 2017). To date, however, research concerning the combined effects of OA and trace metals on molluscan embryos and larvae remains scarce.

Oysters are an important ecosystem component in controlling primary production, maintaining water clarity, providing habitats for benthic organisms and transferring particles from water to sediment (Dame et al. 1989, Ulanowicz & Tuttle 1992, Dame & Libes 1993, Dame 1996). In addition, oysters are an economically important aquaculture species and as such are extensively cultured in China. In 2017, 4 879 422 t, with a value of 5.26 billion USD were harvested in China (www.fao.org). Abalone is also an important aquaculture species, and China accounted for 88.2% of global output in 2017 (www.fao.org).

In the present study, the combined effects of OA and trace metals (Cu and Zn) on embryos and larvae of oysters *C. angulata* and abalone *H. discus hannai* were studied to test whether OA could aggravate trace metal toxicity in molluscs. Oysters and the abalone were selected as study organisms because they are the most widely cultured species along the southern coast of Fujian Province, China. Cu and Zn were used as test trace elements because the 2 metals are the main pollutants in the Jiulong River estu-

ary on the southern coast of Fujian Province (Wang et al. 2011).

2. MATERIALS AND METHODS

2.1. Construction of high-pCO₂ seawater system

The design of the experimental system followed that of a previous study (Guo et al. 2015), with several improvements. The principle of this system is mixing CO₂-enriched air with seawater to produce acidified seawater. Air was supplied from an air compressor (AT3000-120L FINE™) and passed through a freeze dryer (YD-3 YIYANG™), a pressure swing adsorption dryer (YS-3 YIYANG™) and an allochroic silica gel column. To avoid the disturbance of CO₂ produced by human activities in the laboratory air, a pipe was connected with the gas inlet of the air compressor on one end, and the other end was placed in the open air outside the lab. The 2 dryers were used to remove excess water vapor so that valves in the system could not be affected by moisture. The silica gel served as an indicator to ensure that all water vapor was removed. The dried air was conducted through a gas pressure regulator (GR300-08 AIRTAC™) and a filter (GF300-08 AIRTAC™) to stabilize its pressure and remove particles. After that, the air passed through another gas pressure regulator (GPR300-08 AIRTAC™) and a needle valve (LZB-6WB(F) SHUANGHUAN™) to obtain a fixed pressure and flow rate. CO₂ was supplied from a cylinder with a purity of 99.99% and manipulated similarly to air, so CO₂ with a fixed pressure and flow rate was obtained.

Both the air and the CO₂ were conducted into buffering bottles with a Venturi pipe and were well mixed. The mixture of air and CO₂ was divided into 2 parts, one for the experiment and the rest conducted through a bypass where a CO₂ sensor (K30FR SENSEAIR™) and a paperless recorder (NHR7100 HR™) were installed to detect the CO₂ concentration in the system. The paperless recorder received the analog signal from the CO₂ sensor, and the CO₂ concentration was displayed on its panel. When setting the pCO₂ level, a needle valve (TZF-1, Trieder) in the CO₂ line was adjusted to change the CO₂ flow

rate, while that in the air line remained unchanged, until the CO₂ concentration in the recorder reached the target value. Finally, CO₂-enriched air was bubbled into 0.22 μm filtered seawater (FSW) to achieve the required pH level when the gas-liquid equilibration was obtained (Fig. 1).

Four pCO₂ conditions were established: 400 μatm, representing the current ambient atmospheric CO₂ concentration; 800 μatm, representing an intermediate IPCC case scenario of 747 μatm at the end of the 21st century; 1500 μatm, corresponding to the upper limit of the pCO₂ range observed in coastal regions affected by upwelling, including the Peruvian upwelling system (Friederich et al. 2008) and the California Current Ecosystem (Reum et al. 2016); and 2000 μatm, corresponding to the future pCO₂ level of coastal seawater in which acidification is amplified by anthropogenic effects (Melzner et al. 2013) and which has already been used in several studies (e.g. Lopes et al. 2016, Wang et al. 2016). Temperature and pH were measured with a pH meter (Thermo Scientific Orion Star Series™ Benchtop) with a probe (8157BNUMD) calibrated with NBS buffer (4.00, 7.00 and 10.00). A seawater sample (500 ml) was taken from the tank and immediately fixed using 200 μl of saturated mercuric chloride solution. Total alkalinity was determined by Gran acidimetric titration with an Apollo TA Analyzer (Cai & Wang 1998). Salinity was measured with an optical

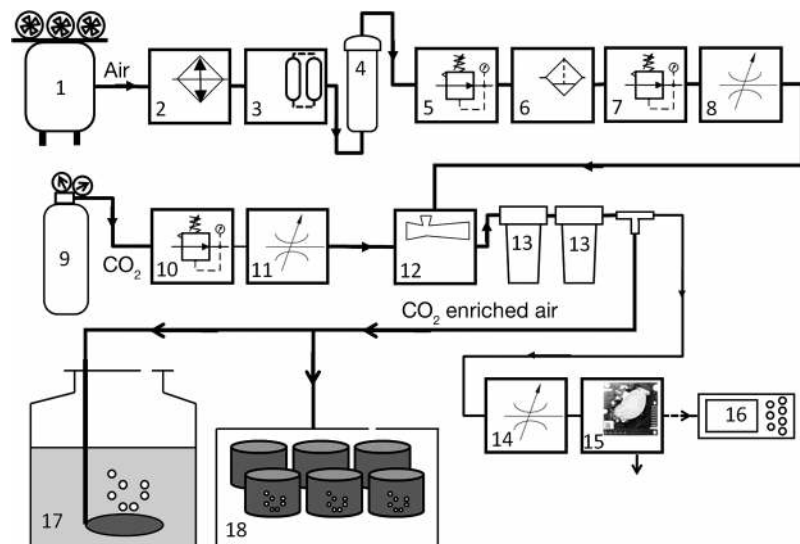


Fig. 1. Schematic of the instrument simulating ocean acidification (OA) for the molluscan larvae experiment. 1: air compressor, 2: freeze dryer, 3: pressure swing adsorption dryer, 4: allochroic silica gel column, 5: gas pressure regulator, 6: air filter, 7: gas pressure regulator, 8: needle valve, 9: CO₂ cylinder, 10: gas pressure regulator, 11: needle valve, 12: venturi pipe, 13: buffering bottles, 14: needle valve, 15: CO₂ sensor, 16: paperless recorder, 17: seawater tank, 18: chamber for larvae culture

salinity meter gauge. Carbonate system parameters were calculated using CO2SYS software (version 2.1). The pH, total alkalinity, temperature, salinity and other calculated data are listed in Table 1.

2.2. Test solutions of metals under different pCO₂ levels

Metals used in tests were from inorganic salts (CuSO₄·5H₂O and ZnSO₄·7H₂O) and were all analytical grade. Stock solutions were made using deionized water and then diluted with filtered seawater of different pCO₂ levels to obtain test solutions with different metal concentrations. Background metal concentrations of Cu and Zn in seawater were measured by the co-precipitation method of Sawatari et al. (1995) and were 0.91 µg l⁻¹ and 6.76 µg l⁻¹, respectively. Nominally, metal concentrations (above the seawater background levels) for the oyster fertilization tests were 0, 10, 20, 50, 80 and 100 µg l⁻¹ for Cu and 0, 1, 2, 3 and 4 µg ml⁻¹ for Zn. Metal concentrations for the oyster larvae tests were 0, 5 and 10 µg l⁻¹ for Cu and 0, 25 and 50 µg l⁻¹ for Zn. Metal concentrations for the abalone fertilization tests were 0, 30, 60, 150, 240 and 300 µg l⁻¹ for Cu and 0, 0.2, 0.5, 1, 2 and 4 µg ml⁻¹ for Zn. Metal concentrations for the abalone larvae tests were 0, 2.5 and 5 µg l⁻¹ for Cu and 0, 20, 40 and 60 µg l⁻¹ for Zn. Metal concentrations used in larvae tests were approximately the same magnitude as those in the polluted sites in the Jiulong River estuary (Cu: 2.84–12.54 µg l⁻¹ and Zn: 4.81–19.92 µg l⁻¹; Weng & Wang 2014). The short duration (~2 h) of fertilization tests allowed only transitory contact between gametes and metals, necessitating the use of higher metal concentrations than environmental levels to ensure an effect. Test solutions were prepared in 100 ml volumetric flasks,

transferred into 100 ml polyethylene (PE) bottles with caps, sealed with parafilm, and stored for the biological tests. Metal concentrations in subsamples of test solutions were also measured, and the data are provided in Table A1 in the Appendix.

2.3. Fertilization and larvae tests for oysters and abalone

Adult oysters and abalone were obtained from FUDA aquaculture farm in Jinjiang, Fujian, China. The molluscs were transferred to the lab and acclimated for 7 d before the experiments, using the culturing method previously reported by Guo et al. (2015).

To obtain eggs and sperm from oysters, oyster shells were opened using an oyster shucker. Individuals with fully developed gonads were selected and put on an enamel tray. A 24-well plate with FSW in each well was used for gamete selection. The gonad was pierced with a 200 µl pipette tip, and a 20 µl aliquot of gametes was removed and transferred into one well of the plate. A new pipette tip was used for each oyster and contact between tips was avoided to prevent undesired fertilization before the test. At 15 min post transfer, gametes in the wells were checked under an inverted microscope (DM IL LED Leica™). Eggs that were mature enough for fertilization were globular or pear-shaped, with a transparent nucleus in the center surrounded by densely packed granules. Suitable sperm were swimming rapidly. Eggs from 3 to 5 oysters were selected, pooled, and used to prepare a dense suspension in FSW. Eggs were then washed 2 to 3 times with FSW to remove undesired gonad debris. Sperm from 3 to 5 oysters were also selected, pooled, and made into a suspension with FSW. To obtain eggs and sperm from abalone, individuals with fully developed gonads were stimulated

Table 1. Mean ± SD of water chemistry measurements and calcite and aragonite saturation state (Ω) of seawater in control and high-pCO₂ groups. n = 3 for all treatments. Parameters such as pCO₂, concentration of CO₂, bicarbonate ions and carbonate ions and Ω were calculated by the CO2SYS software

Parameter	Control	800 µatm	1500 µatm	2000 µatm
Temperature (°C)	24.7 ± 0.1	25.0 ± 0.1	24.4 ± 0.2	24.7 ± 0.3
pH (NBS scale)	8.16 ± 0.02	7.93 ± 0.01	7.69 ± 0.01	7.60 ± 0.02
Alkalinity (µmol kg ⁻¹)	2294.1 ± 1.2	2242.1 ± 0.7	2248.1 ± 0.7	2286.8 ± 2.0
Salinity	30.3 ± 0.5	30.3 ± 0.5	30.3 ± 0.5	30.3 ± 0.5
pCO ₂ (µatm)	423.3	808.3	1480.4	1884.4
[CO ₂] (µmol kg ⁻¹)	12.4	23.4	43.6	55.1
[HCO ₃ ⁻] (µmol kg ⁻¹)	1831.4	1960.2	2079.3	2144.5
[CO ₃ ²⁻] (µmol kg ⁻¹)	191.6	116.4	69.7	59.0
Ω_{cal}	4.78	2.91	1.74	1.47
Ω_{ara}	3.12	1.90	1.13	0.96

with UV-radiated seawater to produce gametes. Viable eggs and sperm were also selected, pooled and made into suspensions with FSW.

A complete 2 fixed factor factorial design was adopted in the biological tests: for example, there were 24 treatments (4 pCO₂ levels × 6 Cu concentrations) in the oyster fertilization test. Each treatment was replicated 4 times, and embryos or larvae were cultured in 40 ml polypropylene (PP) bottles. The bottles were placed in a chamber connected to a pipe that supplied CO₂-enriched air from the system described in Section 2.1 so that a micro-environment with high pCO₂ was maintained; this ensured that the water pH did not vary greatly during the experiment. Four chambers were used for each of the 4 pCO₂ levels, and each chamber contained a series of replicate bottles with different metal concentrations.

For both fertilization and larvae tests, a 20 µl volume of egg suspension and 20 µl of sperm suspension were added to each bottle to initiate fertilization. The volume of gamete suspension was small relative to the total volume of the test solution and had only a minor dilution effect on the metal concentration. Density of eggs in each was maintained at 10 eggs ml⁻¹ for oysters and 2 eggs ml⁻¹ for abalone to minimize the metabolic effects of embryos on the seawater pH, while sperm amounts were adjusted to achieve a concentration of 10³ ml⁻¹ in the test solution. After adding the sperm suspension, the bottles were gently shaken for 10 s and then transferred into the chambers. The chambers were put in a thermo-static incubator with a set temperature of 25°C for oyster and 22°C for abalone. At 30 min after fertilization, the FSW was refreshed several times to remove excess sperm.

At 2 h post-fertilization (hpf), the fertilization test was terminated by adding 20 µl buffered formalin to each bottle. Photos of the resulting embryos for fertilization rate and egg diameter measurements were taken using a CCD camera connected to a microscope (CX31 Olympus™). Fertilization rate (%) was calculated by counting the number of cleaved embryos and the total number of eggs:

$$\text{Fertilization rate} = \left(\frac{\text{no. cleaved embryos}}{\text{no. total eggs}} \right) \times 100 \quad (1)$$

Egg diameter was defined as the sum of the cytoplasm and vitelline layer according to Graham et al. (2006) and was measured with the software Image-Pro Plus 6.0. Egg diameter was observed only for abalone.

At 24 hpf, the larvae test was terminated by adding 20 µl buffered formalin to each bottle. Deformation

and shell length were observed. Deformation rate (%) was calculated following the methods of His et al. (1997) for oysters and Hunt & Anderson (1990) for abalone.

$$\text{Deformation rate} = \left(\frac{\text{no. deformed larvae}}{\text{no. total larvae}} \right) \times 100 \quad (2)$$

Approximately 50 embryos/larvae were randomly sampled from each bottle and observed under the microscope.

All the containers used for solution preparation and biological tests were soaked in 1:10 (v:v) nitric acid for at least 24 h and rinsed with deionized water 3 times before the experiment.

2.4. Statistics

Data on fertilization rate and larval deformation were arcsine and square root transformed to meet the assumption of homogeneity of variance for ANOVA. A 2-way ANOVA was performed with pCO₂ and metal as fixed factors. Simple effects of pCO₂ or metal were analyzed using a 1-way ANOVA with a Student-Newman-Keuls (SNK) post hoc test when interactions of the 2 factors were found. A Kruskal-Wallis (KW) test was applied when data transformations failed to result in homogeneity of variance. Differences were considered significant if $p < 0.05$. All statistical analyses were performed using SPSS v17.0.

3. RESULTS

3.1. Combined effects of OA and trace metals on fertilization of *Crassostrea angulata*

There was an interaction between OA and the effect of Cu on fertilization of *C. angulata* (2-way ANOVA, $F_{15,72} = 95.5$, $p < 0.001$; Table 2). Fertilization was unaffected by rising pCO₂ when no Cu was added (1-way ANOVA, $F_{3,15} = 1.5$, $p = 0.27$); however, fertilization was significantly higher at high pCO₂ than low pCO₂ when Cu addition exceeded 10 µg l⁻¹ (e.g. when 20 µg l⁻¹ of Cu was added, fertilization rate increased 86.1% between 400 and 2000 µatm pCO₂; SNK, $p < 0.001$; Fig. 2a). In other words, the toxicity of Cu to oyster fertilization was alleviated by increasing pCO₂ in seawater.

An interaction also existed between OA and the effect of Zn on oyster fertilization (2-way ANOVA, $F_{12,60} = 12.7$, $p < 0.001$; Table 2), with similar effects to those of the combined OA and

Table 2. Results of 2-way ANOVA examining the combined effects of pCO₂ and trace metals on embryonic and larval development of the oyster *Crassostrea angulata* and abalone *Haliotis discus hannai*. *p < 0.05

Response variable	Source of variance	df	MS	F	p
Fertilization of <i>C. angulata</i>	CO ₂	3	3088.5	439.4	<0.001*
	Cu	5	19046.8	2710.0	<0.001*
	CO ₂ × Cu	15	671.3	95.5	<0.001*
	Residual	72	7.0		
	CO ₂	3	858.9	120.1	<0.001*
	Zn	4	7905.6	1105.2	<0.001*
	CO ₂ × Zn	12	90.9	12.7	<0.001*
	Residual	60	7.2		
Fertilization of <i>H. discus hannai</i>	CO ₂	3	1144.1	42.1	<0.001*
	Cu	5	3980.1	146.6	<0.001*
	CO ₂ × Cu	15	171.8	6.3	<0.001*
	Residual	72	27.2		
	CO ₂	3	426.9	30.6	<0.001*
	Zn	5	21712.5	1556.9	<0.001*
	CO ₂ × Zn	15	168.8	12.1	<0.001*
	Residual	72	13.9		
Egg diameter of <i>H. discus hannai</i>	CO ₂	1	2940.7	87.0	<0.001*
	Cu	2	5345.6	158.2	<0.001*
	CO ₂ × Cu	2	1432.6	42.4	<0.001*
	Residual	18	33.8		
	CO ₂	1	23.6	13.3	<0.001*
	Zn	2	22.9	12.9	<0.001*
	CO ₂ × Zn	2	24.9	14.1	<0.001*
	Residual	18	1.8		
Deformation of <i>C. angulata</i> larvae	CO ₂	2	3719.3	1261.3	<0.001*
	Cu	2	6723.6	2280.1	<0.001*
	CO ₂ × Cu	4	328.5	111.4	<0.001*
	Residual	27	2.9		
	CO ₂	2	1853.3	164.9	<0.001*
	Zn	2	3619.1	322.0	<0.001*
	CO ₂ × Zn	4	30.4	2.7	0.051
	Residual	27	11.2		
Deformation of <i>H. discus hannai</i> larvae	CO ₂	2	1468.7	162.6	<0.001*
	Cu	2	2442.9	270.5	<0.001*
	CO ₂ × Cu	4	441.4	48.9	<0.001*
	Residual	36	9.0		
	CO ₂	2	7860.4	543.2	<0.001*
	Zn	3	3617.9	250.0	<0.001*
	CO ₂ × Zn	6	579.3	40.0	<0.001*
	Residual	27	11.2		
Shell length of <i>C. angulata</i> larvae	CO ₂	2	184.5	104.0	<0.001*
	Cu	2	226.5	127.7	<0.001*
	CO ₂ × Cu	4	3.8	2.1	0.106
	Residual	27	1.8		
	CO ₂	2	255.3	574.5	<0.001*
	Zn	2	35.8	80.6	<0.001*
	CO ₂ × Zn	4	1.7	3.7	0.015*
	Residual	27	0.4		
Shell length of <i>H. discus hannai</i> larvae	CO ₂	2	528.2	30.1	<0.001*
	Cu	2	301.1	17.1	<0.001*
	CO ₂ × Cu	4	205.1	11.7	<0.001*
	Residual	27	17.6		
	CO ₂	2	4183.5	110.2	<0.001*
	Zn	3	9920.3	261.2	<0.001*
	CO ₂ × Zn	6	1098.9	28.9	<0.001*
	Residual	36	38.0		

Cu treatment. Fertilization was unaffected by pCO₂ levels when no Zn was added, while fertilization was significantly higher at high pCO₂ than at low pCO₂ with increasing Zn addition (e.g. when 1 µg ml⁻¹ of Zn was added, fertilization rate increased 26.4% between 400 and 2000 µatm pCO₂: SNK, p < 0.001; Fig. 2b).

3.2. Combined effects of OA and trace metals on fertilization of *Haliotis discus hannai*

There was an interaction between OA and the effect of Cu on fertilization of *H. discus hannai* (2-way ANOVA, $F_{15,72} = 6.3$, p < 0.001; Table 2). For example, fertilization was not significantly different between pCO₂ 400 and 2000 µatm when no Cu was added (1-way ANOVA, $F_{3,15} = 0.49$, p = 0.70; Fig. 3a). However, fertilization was reduced by 34.7% at 2000 µatm when 150 µg l⁻¹ of Cu was added (SNK, p < 0.001; Fig. 3a). Similarly, fertilization was reduced by 33.0% at 1500 µatm when 300 µg l⁻¹ of Cu was added (SNK, p = 0.001; Fig. 3a). In other words, the toxicity of Cu to abalone fertilization was aggravated by increasing pCO₂ in seawater.

In contrast, the toxicity of Zn to abalone fertilization was alleviated by increasing pCO₂, and the interaction of these 2 factors was significant (2-way ANOVA, $F_{15,72} = 12.1$, p < 0.001; Table 2). For example, fertilization was unaffected by pCO₂ level when no (1-way ANOVA, $F_{3,15} = 0.34$, p = 0.80) and 0.2 µg ml⁻¹ (1-way ANOVA, $F_{3,15} = 1.1$, p = 0.40) Zn was added (Fig. 3b); however, fertilization was 43.7% lower at 400 µatm pCO₂ than at 1500 µatm when 1 µg ml⁻¹ Zn was added (SNK, p < 0.001; Fig. 3b).

There were also interactive effects of pCO₂ and metals on egg diameter in abalone (Table 2). Cu addition caused a significant egg diameter in-

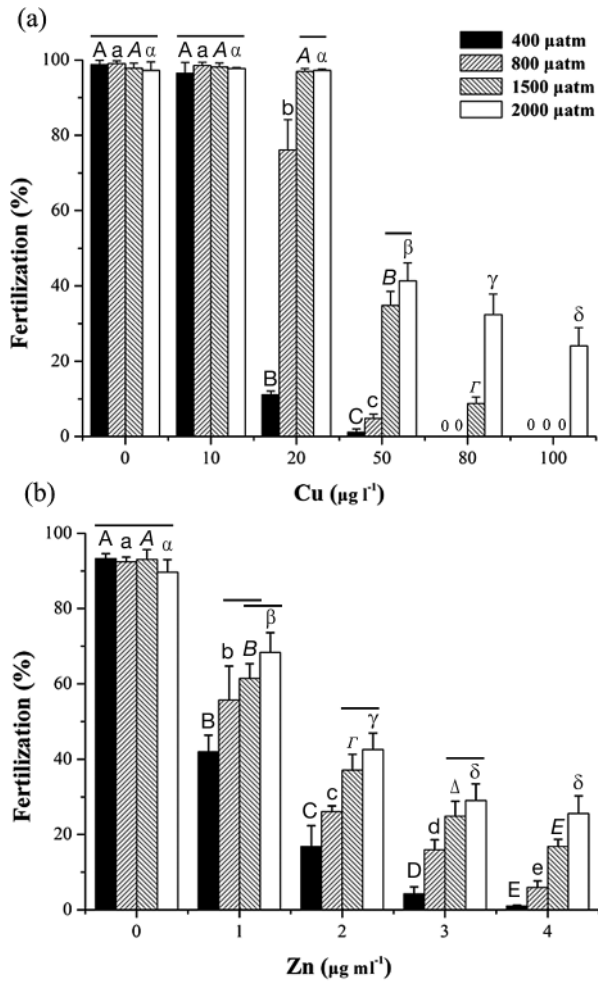


Fig. 2. Fertilization rate (mean + SD, $n = 4$) of *Crassostrea angulata* 2 h post fertilization at 4 levels of $p\text{CO}_2$ with the addition of (a) Cu or (b) Zn. Different upper- and lowercase letters represent significant differences between trace metal concentrations at the same $p\text{CO}_2$ level ($p < 0.05$). A line above columns indicates no significant difference across $p\text{CO}_2$ levels at the same trace metal concentrations. Columns not connected by lines are significantly different from each other ($p < 0.05$)

crease at a $p\text{CO}_2$ level of 400 μatm , yet this effect decreased as $p\text{CO}_2$ increased. For example, at 400 μatm , egg diameter increased by 11.2% when 150 $\mu\text{g l}^{-1}$ Cu was added (SNK, $p < 0.001$; Fig. 4a); however, at 1500 μatm , there was no significant difference in egg diameter between the 0 and 150 $\mu\text{g l}^{-1}$ Cu treatments (SNK, $p = 0.16$; Fig. 4a). Similarly, the average egg diameter increased by 37.8% when 300 $\mu\text{g l}^{-1}$ Cu was added at 400 μatm , but by only 11.6% at 1500 μatm (Fig. 4c). Zn addition had no effect on egg diameter at 400 μatm (1-way ANOVA, $F_{2,11} = 3.9$, $p = 0.061$); however, egg diameter decreased significantly when Zn was added at 1500 μatm (e.g. a 2.5% reduction in diameter with the addition of 1 $\mu\text{g ml}^{-1}$ Zn: SNK, $p < 0.001$; Fig. 4b,d).

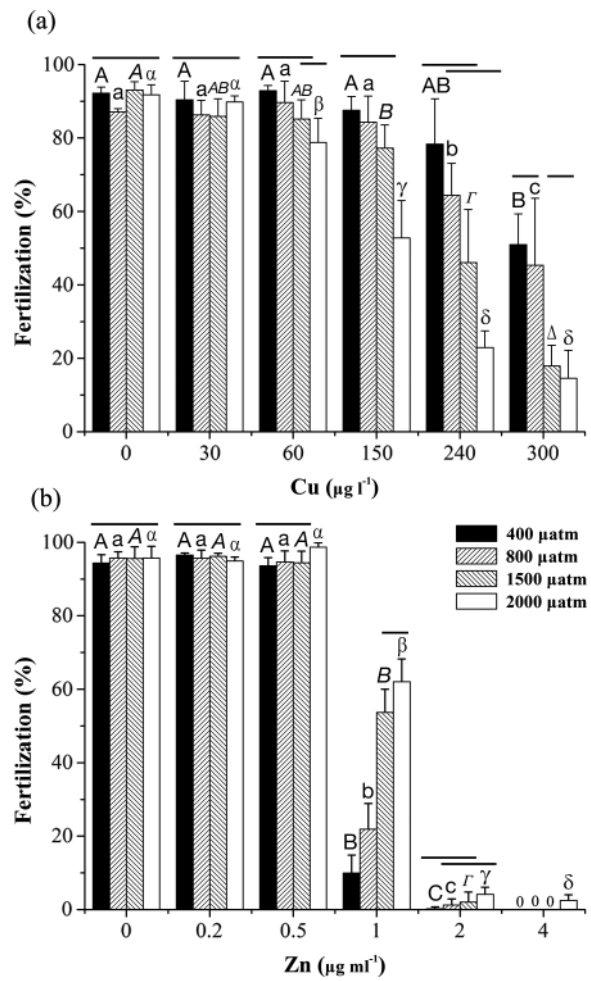


Fig. 3. Fertilization rate (mean + SD, $n = 4$) of *Haliotis discus hannai* 2 h post fertilization at 4 levels of $p\text{CO}_2$ with the addition of (a) Cu or (b) Zn. Different upper- and lowercase letters represent significant differences between trace metal concentrations at the same $p\text{CO}_2$ level ($p < 0.05$). A line above columns indicates no significant difference across $p\text{CO}_2$ levels at the same trace metal concentrations. Columns not connected by lines are significantly different from each other ($p < 0.05$)

3.3. Combined effects of OA and trace metals on larval deformation of *C. angulata*

A significant interaction between the effects of OA and Cu on larval deformation in *C. angulata* was observed (2-way ANOVA, $F_{4,27} = 111.4$, $p < 0.001$; Table 2). For example, the larval deformation rate increased by 7.7% between the no Cu and 5 $\mu\text{g l}^{-1}$ Cu treatments at 400 μatm (SNK, $p < 0.001$; Fig. 5a), but by 22.0% at 800 μatm (SNK, $p < 0.001$; Fig. 5a). Thus, OA increased Cu toxicity to oyster larval development.

In contrast, there was no interaction between the effects OA and Zn in larval deformation of *C. angu-*

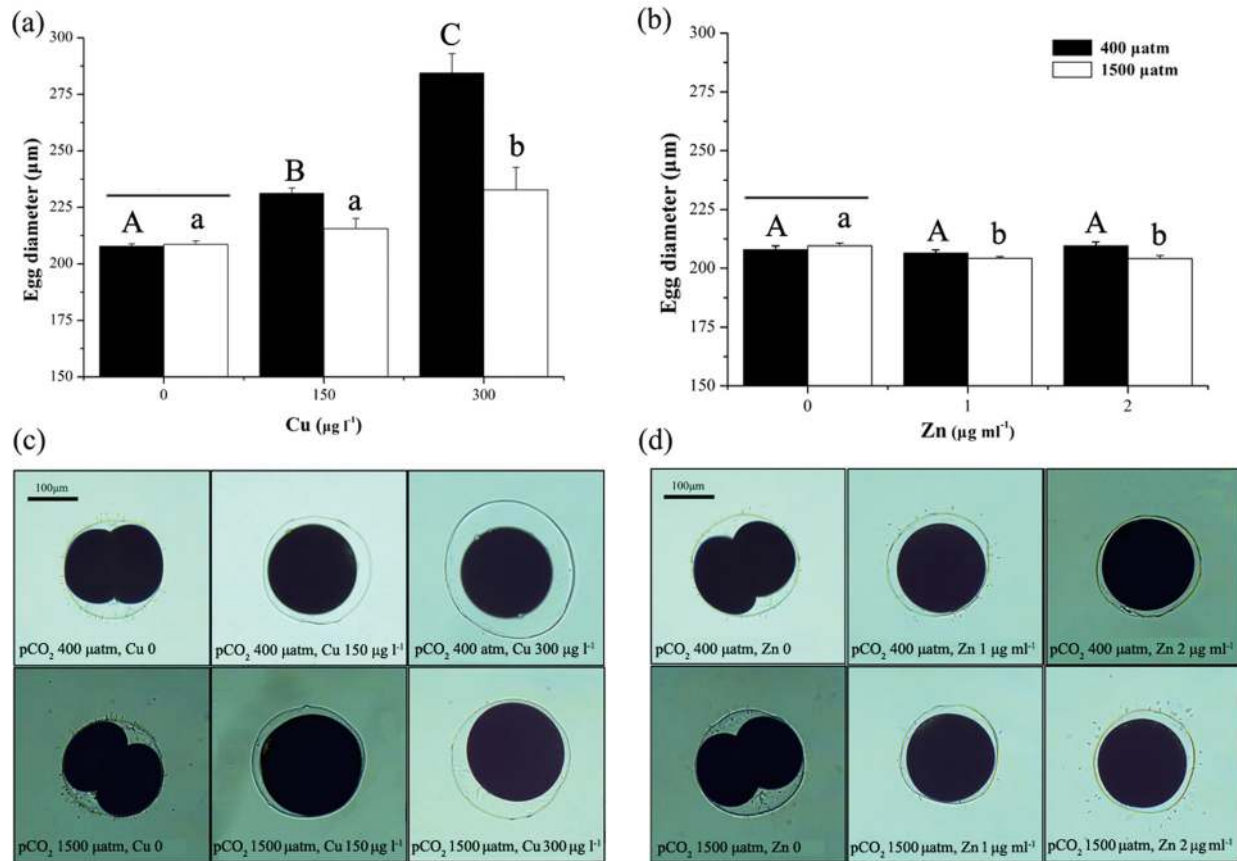


Fig. 4. Egg diameter (mean + SD; $n = 4$) of *Haliotis discus hannai* 2 h post fertilization at pCO₂ 400 and 1500 µatm with the addition of (a) Cu or (b) Zn. Different upper- and lowercase letters represent significant differences between different trace metal concentrations at the same pCO₂ level ($p < 0.05$). A line above columns indicates no significant difference between 400 and 1500 µatm at the same trace metal concentration. Columns not connected by lines are significantly different from each other ($p < 0.05$). Photos showing (c) significant expansion of egg membrane in high Cu concentration treatments at pCO₂ 400 µatm but less evident expansion at pCO₂ 1500 µatm, and (d) subtle but significant reduction of egg diameter in high Zn concentration treatments at pCO₂ 1500 µatm

lata (2-way ANOVA, $F_{4,27} = 2.7$, $p = 0.051$; Table 2, Fig. 5b).

3.4. Combined effects of OA and trace metals on larval deformation of *H. discus hannai*

A significant interaction between the effects of OA and Cu on larval deformation in *H. discus hannai* was detected (2-way ANOVA, $F_{4,36} = 48.9$, $p < 0.001$; Table 2). For example, larval deformation increased by 10.7% between the no Cu and 5 µg l⁻¹ Cu treatments at 400 µatm (SNK, $p = 0.001$; Fig. 6a), but by 71.4% at 1500 µatm (SNK, $p < 0.001$; Fig. 6a). OA thus increased Cu toxicity to abalone larval development.

An interaction also existed between the effects of OA and Zn on larval deformation of *H. discus hannai* (2-way ANOVA, $F_{6,36} = 40.0$, $p < 0.001$; Table 2). For

example, at 400 µatm, larval deformation increased by 31.5% when 60 µg l⁻¹ Zn was added (KW, $p = 0.032$; Fig. 6b); however, at 1500 µatm, deformation increased by 37.2% when only 20 µg l⁻¹ Zn was added (SNK, $p < 0.001$; Fig. 6b). OA increased Zn toxicity to abalone larval development.

3.5. Combined effects of OA and trace metals on larval shell length of *C. angulata*

OA and Cu had no interactive effects on larval shell length in *C. angulata* (2-way ANOVA, $F_{4,27} = 2.1$, $p = 0.11$; Table 2, Fig. 7a). However, an interaction existed between the effects of OA and Zn on shell length (2-way ANOVA, $F_{4,27} = 3.7$, $p = 0.015$; Table 2). For example, shell length was reduced by 3.1% between 0 and 25 µg l⁻¹ Zn at 400 µatm (SNK,

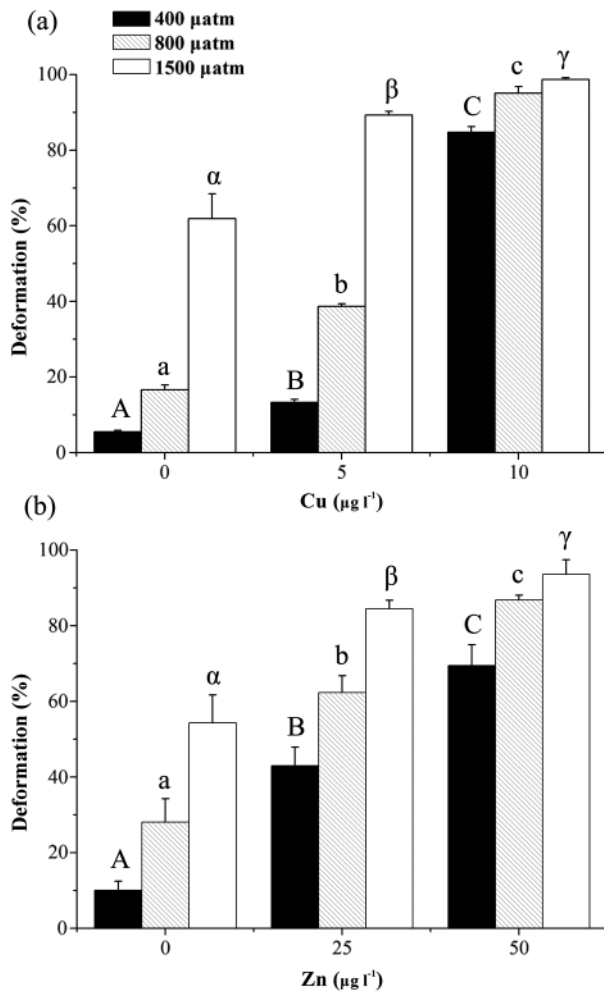


Fig. 5. Deformation rate (mean + SD; $n = 4$) of *Crassostrea angulata* larvae 24 h post fertilization at 3 pCO₂ levels with the addition of (a) Cu or (b) Zn. Different upper- and lowercase letters represent significant differences between trace metal concentrations at the same pCO₂ level ($p < 0.05$). A line above columns indicates no significant difference between pCO₂ levels at the same trace metal concentration. Columns not connected by lines are significantly different from each other ($p < 0.05$)

$p < 0.001$; Fig. 7b), but only by 1.5% at 800 µatm (SNK, $p < 0.001$; Fig. 7b). Overall, OA alleviated Zn inhibition of oyster larval calcification.

3.6. Combined effects of OA and trace metals on larval shell length of *H. discus hannai*

There was an interaction between the effects of OA and Cu on larval shell length in *H. discus hannai* (2-way ANOVA, $F_{4,27} = 11.7$, $p < 0.001$; Table 2). For example, shell length did not change with rising Cu concentration at 400 µatm (1-way ANOVA, $F_{2,11} =$

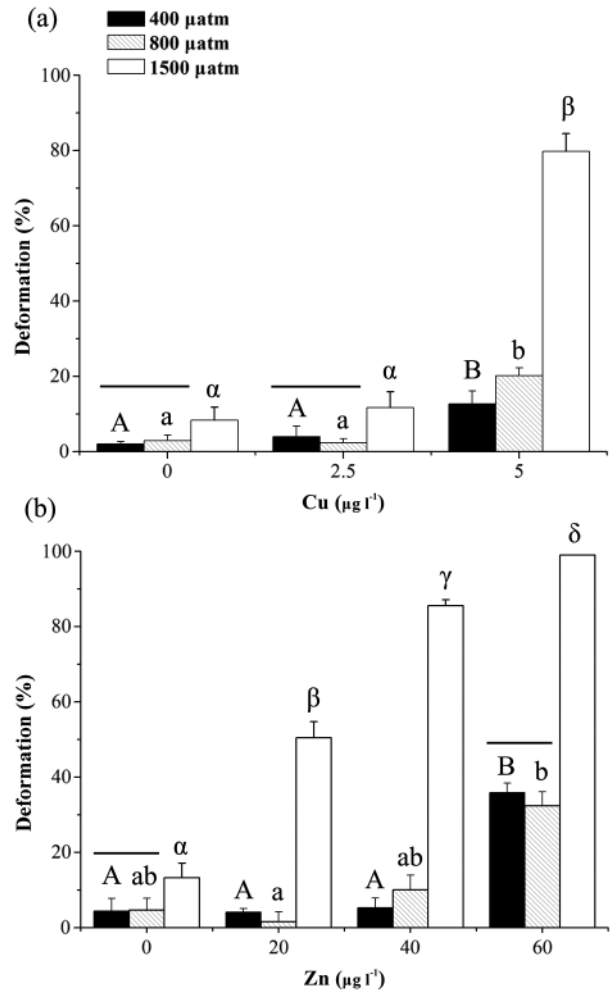


Fig. 6. Deformation rate (mean + SD; $n = 4$) of *Haliotis discus hannai* larvae 24 h post fertilization at 3 pCO₂ levels with the addition of (a) Cu or (b) Zn. Different upper- and lowercase letters represent significant differences between trace metal concentrations at the same pCO₂ level ($p < 0.05$). A line above columns indicates no significant difference between pCO₂ levels at the same trace metal concentration. Columns not connected by lines are significantly different from each other ($p < 0.05$)

0.21, $p = 0.82$; Fig. 8a) and 800 µatm (1-way ANOVA, $F_{2,11} = 1.9$, $p = 0.20$; Fig. 8a). However, at 1500 µatm, shell length was reduced by 8.8% when 5 µg l⁻¹ Cu was added (SNK, $p = 0.001$, Fig. 8a).

An interaction also existed between the effects of OA and Zn on shell length in *H. discus hannai* (2-way ANOVA, $F_{6,36} = 28.9$, $p < 0.001$; Table 2). For example, at 400 and 800 µatm, shell length decreased by 8.1% (SNK, $p < 0.001$, Fig. 8b) and 6.6% (SNK, $p < 0.001$, Fig. 8b) respectively when 60 µg l⁻¹ Zn was added. However, at 1500 µatm, shell length was reduced by 8.6% when only 20 µg l⁻¹ Zn was added (SNK, $p < 0.001$, Fig. 8b).

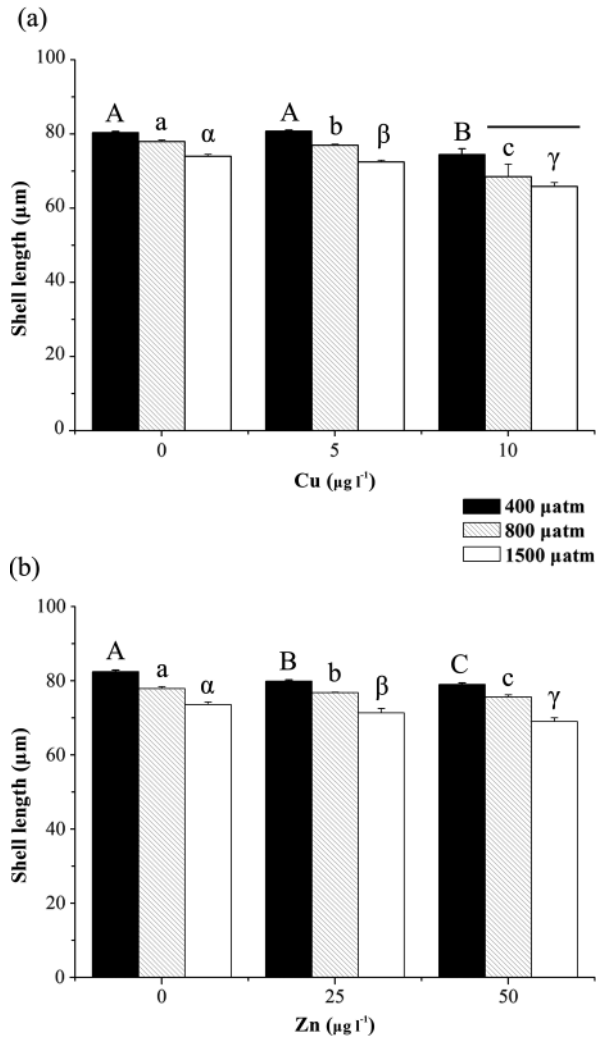


Fig. 7. Shell length (mean + SD; n = 4) of *Crassostrea angulata* larvae 24 h post fertilization at 3 pCO₂ levels with the addition of (a) Cu or (b) Zn. Different upper- and lowercase letters represent significant differences between trace metal concentrations at the same pCO₂ level (p < 0.05). A line above columns indicates no significant difference between pCO₂ levels at the same trace metal concentration. Columns not connected by lines are significantly different from each other (p < 0.05)

4. DISCUSSION

Inhibition of fertilization under high-pCO₂ conditions occurs in different marine invertebrates (Morita et al. 2010, Moulin et al. 2011, Reuter et al. 2011, Barros et al. 2013, Foo et al. 2014). In the marine bivalve *Tegillarca granosa*, sperm motility, gamete fusion and ovular calcium oscillation in fertilization were all impeded by OA (Shi et al. 2017). Respiration of sperm was inhibited in the mussel *Mytilus edulis* at pH < 7.5 (Akberali et al. 1985). Similarly, the mitochondrial membrane potential (MMP) in sperm of the sea

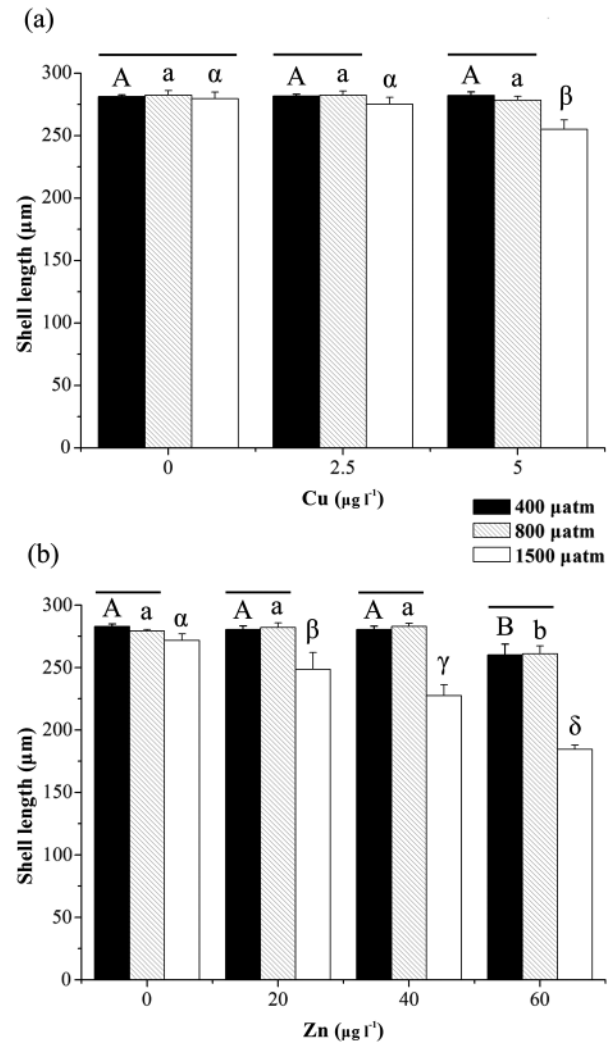


Fig. 8. Shell length (mean + SD; n = 4) of *Haliotis discus hannai* larvae 24 h post fertilization at 3 pCO₂ levels with the addition of (a) Cu or (b) Zn. Different upper- and lowercase letters represent significant differences between trace metal concentrations at the same pCO₂ level (p < 0.05). A line above columns indicates no significant difference between pCO₂ levels at the same trace metal concentration. Columns not connected by lines are significantly different from each other (p < 0.05)

urchin *Centrostephanus rodgersii* was significantly reduced under OA conditions (pH reduced by 0.3 and 0.5; Schlegel et al. 2015). The main energy source for motility in sperm is mitochondrial respiration, for which MMP can be used as a proxy; sperm in ambient seawater usually have a higher MMP than sperm in high-pCO₂ seawater. Consequently, the reduced motility of sperm under OA conditions could be the result of inhibited respiration. The acrosome reaction and ovular calcium oscillation are crucial processes for gamete fusion and embryo development respectively, and both require an influx of cal-

cium into gametes. Since OA may lead to reduced intracellular pH (Gibbin et al. 2014), which prevents calcium uptake by the cell from seawater (Thomas & Meech 1982), the overall result may be failure of both the acrosome reaction and embryo cleavage.

Adverse effects of Cu and Zn on fertilization have often been reported (Reichelt-Brushett & Harrison 1999, Reichelt-Brushett & Michalek-Wagner 2005, Victor & Richmond 2005). Cu^{2+} is reduced to Cu^+ after entering the cell, which binds with sulfhydryl groups (Viarengo et al. 1996) of enzymes in the electron transport chain (Ay et al. 1999). This can inhibit the ATP production of sperm and affect sperm motility. Cu accumulation in sperm mitochondria can decrease MMP and cause formation of reactive oxygen species (ROS), leading to oxidative damage (Krumnschnabel et al. 2005). Similarly, ROS production is the main toxic effect caused by Zn, which has been observed in many species, including bivalves (Geret & Bebianno 2004). Trace metals may also induce the release of free calcium in eggs from intracellular calcium stores such as the endoplasmic reticulum, causing an increase of intracellular calcium concentration. Fertilized eggs of the sea urchin *Psammechinus miliaris* treated with Cu exhibited a significantly higher free calcium signal than control, untreated eggs (Schäfer et al. 2009). However, the abnormally high calcium concentration significantly inhibited fertilization because degradative enzymes that depended on excess calcium were activated, which compromised mitochondrial function and cytoskeletal organization, and ultimately resulted in developmental failure.

In contrast, Cu and Zn may also have positive effects on molluscan reproduction, e.g. by increasing the ionic permeability of organelle membranes. A significant decrease in calcium level was found in the acrosomes and mitochondria of *M. edulis* sperm after Cu and Zn exposure (Earnshaw et al. 1986). Both metals can induce the release of pre-loaded calcium from the matrix of *M. edulis* mitochondria, with Cu being more effective at this than Zn (Akberali & Earnshaw 1982). The result of this induction could be an increase in the concentration of free calcium in sperm cytoplasm. As intracellular free calcium plays an important role in activating sperm, Cu and Zn may cause an increase in sperm mobility. Likewise, exposure to Cu stimulated the respiration of unfertilized eggs of *M. edulis*, which was attributed to enhanced potassium influx and uncoupling of oxidative phosphorylation induced by Cu (Akberali et al. 1984). Considering respiration of fertilized eggs continues to increase throughout embryonic development, stimulation of respiration by Cu may benefit the develop-

ment of molluscan embryos. Consequently, the effects of Cu and Zn on gametes of marine invertebrates are complex: toxicity to enzymes, production of ROS and excess calcium intake could hamper fertilization, while enhanced gamete respiration could benefit fertilization and embryonic development. Final effects of the 2 metals are likely exposure-dependent, both in terms of duration and concentration.

Under the combined OA and addition of Cu or Zn, metal ions promote calcium influx into the gametes, which could increase sperm velocity, stimulate the acrosomal reaction and also compensate for the insufficient uptake of calcium during fertilization caused by OA. These processes could reduce the adverse effects caused by OA and metals independently, which may be the reason for the antagonistic interaction between the effects of OA and Cu or Zn on fertilization seen in the present study. An alternative explanation is the competition between protons and metal ions for binding sites on the cell surface (Kerndorff & Schnitzer 1980, Schubauer-Berigan et al. 1993). When pCO_2 increases (inducing a higher seawater proton concentration), excess protons may bind to the sperm cell surface, increasing the positive charge on the outer cell membrane and inhibiting the entry of positively charged metal ions. Thus, low pH may represent a protection mechanism for invertebrate reproduction in metal-polluted sites.

In contrast to the antagonistic interaction observed in the combined treatments of OA and metals on oyster fertilization in the present study, rising pCO_2 could increase the toxicity of Cu to abalone fertilization, and this may be attributed to the structure of the abalone egg. Abalone eggs differ from those of oysters in that they are covered with an egg jelly coat and vitelline envelope, with the vitelline envelope beneath the jelly coat. The thickness of the egg jelly varies from 30 to 100 μm for different abalone species, while the vitelline envelope is thin (about 1 μm). The egg jelly of abalone *Haliotis asinina* mainly contains 2 glycoproteins at 107 kDa and 178 kDa, with glucose as the major sugar component, and the vitelline envelope also contains the 2 glycoproteins (Suphamungmee et al. 2010). The role of the egg jelly glycoproteins is to accelerate sperm motility (Suphamungmee et al. 2010), and the vitelline envelope binds with sperm and triggers the acrosome reaction (Vacquier et al. 1999).

Influence of metal ions on the egg jelly and vitelline envelope of marine invertebrates has not been documented. However, a study on the plant cell wall led to the hypothesis that Cu^{2+} could be reduced to Cu^+ by apoplastic electron donors when it complexes with cell wall glycoproteins and that the Cu^+ can

then undergo a Fenton reaction with apoplastic hydrogen peroxide (H_2O_2) to generate hydroxyl radicals ($\cdot\text{OH}$) (Fry et al. 2002). These radicals can cause non-enzymic scission of wall polysaccharides and may loosen the cell wall. Considering the high oxidative capacity of $\cdot\text{OH}$, the structure of the glycoproteins in the egg jelly and vitelline envelope could also be comprised under Cu exposure. Thus, both the egg jelly and the vitelline envelope may lose their integrity due to structural destruction, causing the vitelline envelope to expand, as indicated by the significant increase of egg diameter seen in our experiments. Fertilization success could be improved as a result of the larger surface area for sperm to come in contact with, thus increasing the chance that a sperm cell enters the egg. In other words, Cu may not only be toxic but may also promote abalone fertilization under ambient pCO_2 conditions. Thus, a nearly 50% fertilization rate was maintained in abalone at ambient pCO_2 when as much as $300 \mu\text{g l}^{-1}$ Cu was added, compared with no fertilization in oysters (where egg diameter was not affected) under a Cu addition of $100 \mu\text{g l}^{-1}$ at ambient pCO_2 . In seawater with higher pCO_2 , expansion of the egg membrane was significantly inhibited; therefore, the toxicity of Cu played a more important role. In other words, Cu toxicity to abalone fertilization was enhanced by OA. The subtle but significant reduction of abalone egg diameter under combined treatments of high pCO_2 and Zn addition also indicated that Zn ions might alter egg structure at higher pCO_2 . Further studies are needed to reveal the mechanism of the combined effects of OA and metal ions on abalone egg structure.

Cu addition at high- pCO_2 levels significantly increased larval deformation in oysters in our study. Strong interactions between pCO_2 and Cu were also found by Lewis et al. (2013), where very high polychaete larval mortality occurred at low pH with Cu addition compared to low pH without Cu. This synergistic effect may be attributed to an increase of free Cu and Zn ions under OA, as predicted by Millero et al. (2009). Such a phenomenon was observed by Shi et al. (2016), who found that the ratio of Cd^{2+} to Ca^{2+} was significantly increased in high pCO_2 seawater. In addition, OA could reduce larval metabolic rate, so that the energy supply may become insufficient for larvae to expel trace metals extracellularly. Although OA temporarily inhibits metal ions from penetrating the embryo at the fertilization stage through higher proton concentration, it is highly likely that the metals could still accumulate inside the cell over longer exposure. A recent study found that Cu accumulation was significantly higher in adult oysters exposed to

Cu for 28 d at pH 7.6 than in exposed individuals at pH 8.1 and 7.8 (Cao et al. 2019). Metallothionein (MT) plays an important part in the detoxification of many trace metals in molluscs, and transcription of MT-mRNA can be rapidly activated under metal exposure, leading to increased synthesis of MT which in turn binds metal ions (Isani et al. 2000). However, molluscan embryos might be relatively weak in dealing with metal toxicity. The oyster *Crassostrea virginica* was unable to produce metallothionein before 8 hpf (Roesijadi et al. 1996), and MT-mRNA expression was limited in the larval stage compared to adults (Unger & Roesijadi 1996). Consequently, higher metal accumulation induced by OA and limited detoxification ability during the larval stage could be the reasons for the synergistic effect of OA and metals on larval deformation.

Both Cu and Zn could adversely affect larval shell formation. Cu inhibits the activity of carbonic anhydrase (Vitale et al. 1999), a key enzyme in organism calcification, thus reducing shell growth. Decreased shell growth under Zn exposure might be caused by its competitive binding with calcium receptors when the shell is forming, as the Zn and Ca ions have similar atomic diameters and are both divalent ions. OA could also modulate gene expression of carbonic anhydrase. Todgham & Hofmann (2009) found an up-regulation of the carbonic anhydrase gene under high pCO_2 , while Stumpp et al. (2011) reported a downward regulation in echinoderm larvae. Suppression of gene expression of carbonic anhydrase was also discovered in larvae of oysters *C. gigas* under high pCO_2 (De Wit et al. 2018). In the present study, the inhibition of abalone larval calcification induced by Cu and Zn was enhanced under OA conditions. OA may have inhibited carbonic anhydrase synthesis in abalone larvae so that more energy was diverted to detoxification of metals. Therefore, the energy was insufficient to sustain normal calcification, and larval shell growth was even more reduced when OA and metals co-occurred. In contrast to abalone, oyster larvae might allocate more energy to maintaining shell growth, and that is why their larval shell growth was not further inhibited under the combined treatment of OA and Cu. Zn ions are cofactors of carbonic anhydrase, and Zn addition might therefore induce the up-regulation of the carbonic anhydrase gene, therefore alleviating inhibition of larval shell growth caused by OA.

Acclimation to environmental changes can be assessed in transgenerational investigations. Exposing adult Sydney rock oysters *Saccostrea glomerata* to high pCO_2 conditions induced parental carryover ef-

fects in the next-generation larvae (Parker et al. 2012). Larvae from oysters undergoing conditioning within elevated pCO₂ environments grew faster and larger than larvae produced by adults raised in ambient pCO₂. Mussel *M. edulis* larvae originating from high pCO₂ environments exhibited increased tolerance to acidified environments (Thomsen et al. 2017). In another study on *M. edulis*, transgenerational exposure to high pCO₂ conditions induced the offspring to precipitate calcite—which is a less soluble form of calcium carbonate—instead of aragonite in their shells (Fitzer et al. 2014). Therefore, molluscs likely become tolerant to OA after long term and transgenerational exposure to low pH conditions. Our study species vary in their likelihood to adapt to OA. *C. angulata* is an estuarine intertidal species that lives in environments with large fluctuations in pH and trace metal concentrations, and has adapted to the unstable environmental conditions over generations of acclimation. Abalone *H. discus hannai* inhabit environmentally stable offshore regions and are thus more susceptible to a changing environment. This may be the reason why our results show *C. angulata* to be more tolerant to the combined effects of OA and metals than *H. discus hannai*. The larval stage is very important for population sustainability of molluscs, and impaired larvae would no doubt reduce the yield of molluscan aquaculture. It is very likely that culture of *H. discus hannai* would be threatened under the concurrence of OA and trace metal pollution at aquaculture sites. Larvae of *C. angulata* seem more resistant to OA and metal in their early developmental stage; however, chronic effects could emerge under longer exposure (e.g. during the entire larval stage or even to the adult stage). Therefore, culture of *C. angulata* could also be adversely affected by combined exposure to OA and metals at oyster farms.

In conclusion, this study has provided evidence that variation in pCO₂ levels, developmental stages, egg structure and species can all affect metal toxicity to the early development of molluscs. Future research should include additional parameters such as other environmental stressors, developmental stages and gamete properties of the tested organisms when assessing metal toxicity to molluscan embryos. Further biochemical and physiological studies are needed to clarify the biological mechanisms of the combined effects of OA and trace metals on molluscan embryonic and larval development. Based on the results of the present study, we propose that the production yield of molluscan aquaculture will decrease at metal polluted sites when seawater becomes more acidic as predicted by climate change models.

Acknowledgements. This study was funded by NSFC (No. 31672651, No. 41176113), Major Science and Technology Projects in Fujian Province (2016NZ0001-4), the Earmarked Fund for Modern Agro-industry Technology Research System (No. CARS-49) and the Quanzhou City Science & Technology Program of China (2018N006).

LITERATURE CITED

- ✦ Akberali HB, Earnshaw MJ (1982) A possible role for mitochondrial calcium in the contraction of the mollusc siphon induced by copper. *Comp Biochem Physiol C Comp Pharmacol* 73:395–398
- ✦ Akberali HB, Earnshaw MJ, Marriott KR (1984) The action of heavy metals on the gametes of the marine mussel, *Mytilus edulis* (L.)—I. Copper-induced uncoupling of respiration in the unfertilized egg. *Comp Biochem Physiol C Comp Pharmacol* 77:289–294
- ✦ Akberali HB, Earnshaw MJ, Marriott KRM (1985) The action of heavy metals on the gametes of the marine mussel, *Mytilus edulis* (L.)—II. Uptake of copper and zinc and their effect on respiration in the sperm and unfertilized egg. *Mar Environ Res* 16:37–59
- ✦ Ay O, Kalay M, Tamer L, Canli M (1999) Copper and lead accumulation in tissues of a freshwater fish *Tilapia zillii* and its effects on the branchial Na, K-ATPase activity. *Bull Environ Contam Toxicol* 62:160–168
- ✦ Barros P, Sobral P, Range P, Chicharo L, Matias D (2013) Effects of seawater acidification on fertilization and larval development of the oyster *Crassostrea gigas*. *J Exp Mar Biol Ecol* 440:200–206
- ✦ Belivermiş M, Warnau M, Metian M, Oberhänsli F, Teyssié JL, Lacoue-Labarthe T (2016) Limited effects of increased CO₂ and temperature on metal and radionuclide bioaccumulation in a sessile invertebrate, the oyster *Crassostrea gigas*. *ICES J Mar Sci* 73:753–763
- Byrne M (2010) Impact of climate change stressors on marine invertebrate life histories with a focus on the Mollusca and Echinodermata. In: Yu J, Henderson-Sellers A (eds) *Climate alert: climate change monitoring and strategy*. University of Sydney Press, Sydney, p 142–185
- Byrne M (2011) Impact of ocean warming and ocean acidification on marine invertebrate life history stages: vulnerabilities and potential for persistence in a changing ocean. *Oceanogr Mar Biol Annu Rev* 49:1–42
- ✦ Byrne M (2012) Global change ecotoxicology: identification of early life history bottlenecks in marine invertebrates, variable species responses and variable experimental approaches. *Mar Environ Res* 76:3–15
- ✦ Cai WJ, Wang Y (1998) The chemistry, fluxes, and sources of carbon dioxide in the estuarine waters of the Satilla and Altamaha Rivers, Georgia. *Limnol Oceanogr* 43:657–668
- ✦ Cai WJ, Hu XP, Huang WJ, Murrell MC and others (2011) Acidification of subsurface coastal waters enhanced by eutrophication. *Nat Geosci* 4:766–770
- ✦ Calabrese A, MacInnes JR, Nelson DA, Miller JE (1977) Survival and growth of bivalve larvae under heavy-metal stress. *Mar Biol* 41:179–184
- ✦ Cao R, Zhang T, Li X, Zhao Y and others (2019) Seawater acidification increases copper toxicity: a multi-biomarker approach with a key marine invertebrate, the Pacific oyster *Crassostrea gigas*. *Aquat Toxicol* 210:167–178
- ✦ Dailianis S, Piperakis SM, Kaloyianni M (2005) Cadmium effects on ROS production and DNA damage via adrenergic receptors stimulation: role of Na⁺/H⁺ exchanger

- and PKC. *Free Radic Res* 39:1059–1070
- Dame RF (1996) Ecology of marine bivalves: an ecosystem approach. CRC Press, Boca Raton, FL
- ✦ Dame RD, Libes S (1993) Oyster reefs and nutrient retention in tidal creeks. *J Exp Mar Biol Ecol* 171:251–258
- ✦ Dame RD, Spurrier JD, Wolaver TG (1989) Carbon, nitrogen and phosphorus processing by an oyster reef. *Mar Ecol Prog Ser* 54:249–256
- ✦ De Wit P, Durland E, Ventura A, Langdon CJ (2018) Gene expression correlated with delay in shell formation in larval Pacific oysters (*Crassostrea gigas*) exposed to experimental ocean acidification provides insights into shell formation mechanisms. *BMC Genomics* 19:160
- ✦ Dupont S, Ortega-Martinez O, Thorndyke M (2010) Impact of near-future ocean acidification on echinoderms. *Ecotoxicology* 19:449–462
- ✦ Earnshaw MJ, Wilson S, Akberali HB, Butlera RD, Marriott KRM (1986) The action of heavy metals on the gametes of the marine mussel, *Mytilus edulis* (L.)—III. The effect of applied copper and zinc on sperm motility in relation to ultrastructural damage and intracellular metal localization. *Mar Environ Res* 20:261–278
- ✦ Fitzer SC, Caldwell GS, Clare AS, Upstill-Goddard RC, Bentley MG (2013) Response of copepods to elevated pCO₂ and environmental copper as co-stressors—a multi-generational study. *PLOS ONE* 8:e71257
- ✦ Fitzer SC, Cusack M, Phoenix VR, Kamenos NA (2014) Ocean acidification reduces the crystallographic control in juvenile mussel shells. *J Struct Biol* 188:39–45
- ✦ Foo SA, Dworjanyan SA, Khatkar MS, Poore AGB, Byrne M (2014) Increased temperature, but not acidification, enhances fertilization and development in a tropical urchin: potential for adaptation to a tropicalized eastern Australia. *Evol Appl* 7:1226–1237
- ✦ Friederich GE, Ledesma J, Ulloa O, Chavez FP (2008) Air-sea carbon dioxide fluxes in the coastal southeastern tropical Pacific. *Prog Oceanogr* 79:156–166
- ✦ Fry SC, Miller JG, Dumville JC (2002) A proposed role for copper ions in cell wall loosening. *Plant Soil* 247:57–67
- ✦ Gattuso JP, Magnan A, Billé R, Cheung WWL and others (2015) Contrasting futures for ocean and society from different anthropogenic CO₂ emissions scenarios. *Science* 349:aac4722
- ✦ Gazeau F, Parker L, Comeau S, Gattuso JP and others (2013) Impacts of ocean acidification on marine shelled mollusks. *Mar Biol* 160:2207–2245
- ✦ Geret F, Bebianno MJ (2004) Does zinc produce reactive oxygen species in *Ruditapes decussatus*? *Ecotoxicol Environ Saf* 57:399–409
- ✦ Geret F, Serafim A, Barreira L, Bebianno MJ (2002) Effect of cadmium on antioxidant enzyme activities and lipid peroxidation in the gills of the clam *Ruditapes decussates*. *Biomarkers* 7:242–256
- ✦ Gibbin EM, Putnam HM, Davy SK, Gates RD (2014) Intracellular pH and its response to CO₂-driven seawater acidification in symbiotic versus non-symbiotic coral cells. *J Exp Biol* 217:1963–1969
- ✦ Gorski J, Nugegoda D (2006) Sublethal toxicity of trace metals to larvae of the blacklip abalone, *Haliotis rubra*. *Environ Toxicol Chem* 25:1360–1367
- ✦ Götze S, Matoo OB, Beniash E, Saborowski R, Sokolova IM (2014) Interactive effects of CO₂ and trace metals on the proteasome activity and cellular stress response of marine bivalves *Crassostrea virginica* and *Mercenaria mercenaria*. *Aquat Toxicol* 149:65–82
- ✦ Graham F, Mackrill T, Davidson M, Daume S (2006) Influence of conditioning diet and spawning frequency on variation in egg diameter for greenlip abalone, *Haliotis laevis*. *J Shellfish Res* 25:195–200
- ✦ Guo X, Huang M, Pu F, You W, Ke C (2015) Effects of ocean acidification caused by rising CO₂ on the early development of three mollusks. *Aquat Biol* 23:147–157
- ✦ Heuer RM, Grosell M (2014) Physiological impacts of elevated carbon dioxide and ocean acidification on fish. *Am J Physiol Regul Integr Comp Physiol* 307:R1061–R1084
- ✦ His E, Seaman MNL, Beiras R (1997) A simplification of the bivalve embryogenesis and larval development bioassay method for water quality assessment. *Water Res* 31:351–355
- Hunt JW, Anderson BS (1990) Abalone larval development: short-term toxicity test protocol. In: Anderson BW, Hunt JW, Turpen SL, Coulon AR, Martin M, McKeown DL, Palmer FH (eds) Procedures manual for conducting toxicity tests developed by the marine bioassay project. California State Water Resources Control Board, Sacramento, CA, p 17–48
- ✦ Isani G, Andreani G, Kindt M, Carpenè E (2000) Metallothioneins (MTs) in marine mollusks. *Cell Mol Biol* 46:311–330
- ✦ Ivanina AV, Beniash E, Eitzkorn M, Meyers TB, Ringwood AH, Sokolova IM (2013) Short-term acute hypercapnia affects cellular responses to trace metals in the hard clams *Mercenaria mercenaria*. *Aquat Toxicol* 140–141:123–133
- ✦ Johnson D (1988) Development of *Mytilus edulis* embryos: a bioassay for polluted waters. *Mar Ecol Prog Ser* 46:135–138
- ✦ Kerndorff H, Schnitzer M (1980) Sorption of metals on humic acid. *Geochim Cosmochim Acta* 44:1701–1708
- ✦ Kroeker KJ, Kordas RI, Crim RM, Hendriks IE and others (2013) Impacts of ocean acidification on marine organisms: quantifying sensitivities and interaction with warming. *Glob Change Biol* 19:1884–1896
- ✦ Krumschnabel G, Manzl C, Berger C, Hofer B (2005) Oxidative stress, mitochondrial permeability transition, and cell death in Cu-exposed trout hepatocytes. *Toxicol Appl Pharmacol* 209:62–73
- ✦ Lacoue-Labarthe T, Martin S, Oberhänsli F, Teyssié JL, Markich S, Jeffree R, Bustamante P (2009) Effects of increased pCO₂ and temperature on trace element (Ag, Cd and Zn) bioaccumulation in the eggs of the common cuttlefish *Sepia officinalis*. *Biogeosciences* 6:2561–2573
- ✦ Lewis C, Clemow K, Holt WV (2013) Metal contamination increases the sensitivity of larvae but not gametes to ocean acidification in the polychaete *Pomatoceros lamarckii* (Quatrefages). *Mar Biol* 160:2089–2101
- ✦ Li Y, Wang WX, Wang M (2017) Alleviation of mercury toxicity to a marine copepod under multigenerational exposure by ocean acidification. *Sci Rep* 7:324
- ✦ Lindsey R (2020) Climate change: atmospheric carbon dioxide. www.climate.gov/news-features/understanding-climate/climate-change-atmospheric-carbon-dioxide
- ✦ Lopes AF, Morais P, Pimentel M, Rosa R, Munday PL, Gonçalves EJ, Faria AM (2016) Behavioural lateralization and shoaling cohesion of fish larvae altered under ocean acidification. *Mar Biol* 163:243
- ✦ Martelli A, Rousselet E, Dycke C, Bouron A, Moulis JM (2006) Cadmium toxicity in animal cells by interference with essential metals. *Biochimie* 88:1807–1814
- ✦ Melzner F, Thomsen J, Koeve W, Oschlies A and others (2013) Future ocean acidification will be amplified by hypoxia in coastal habitats. *Mar Biol* 160:1875–1888
- ✦ Millero FJ, Woosley R, Ditrolio B, Waters J (2009) Effect of ocean acidification on the speciation of metals in seawater. *Oceanography* 22:72–85

- ✦ Morita M, Suwa R, Iguchi A, Nakamura M, Shimada K, Sakai K, Suzuki A (2010) Ocean acidification reduces sperm flagellar motility in broadcast spawning reef invertebrates. *Zygote* 18:103–107
- ✦ Moulin L, Catarino AI, Claessens T, Dubois P (2011) Effects of seawater acidification on early development of the intertidal sea urchin *Paracentrotus lividus* (Lamarck 1816). *Mar Pollut Bull* 62:48–54
- ✦ Pan K, Wang WX (2012) Trace metal contamination in estuarine and coastal environments in China. *Sci Total Environ* 421–422:3–16
- ✦ Parker LM, Ross PM, O'Connor WA, Borysko L, Raftos DA, Pörtner HO (2012) Adult exposure influences offspring response to ocean acidification in oysters. *Glob Change Biol* 18:82–92
- ✦ Pascal PY, Fleeger JW, Galvez F, Carman KR (2010) The toxicological interaction between ocean acidity and metals in coastal meiobenthic copepods. *Mar Pollut Bull* 60:2201–2208
- ✦ Reichelt-Brushett AJ, Harrison PL (1999) The effect of copper, zinc and cadmium on fertilization success of gametes from scleractinian reef corals. *Mar Pollut Bull* 38:182–187
- ✦ Reichelt-Brushett AJ, Michalek-Wagner K (2005) Effects of copper on the fertilization success of the soft coral *Lobophytum compactum*. *Aquat Toxicol* 74:280–284
- ✦ Reum JCP, Alin SR, Harvey CJ, Bednaršek N and others (2016) Interpretation and design of ocean acidification experiments in upwelling systems in the context of carbonate chemistry co-variation with temperature and oxygen. *ICES J Mar Sci* 73:582–595
- ✦ Reuter KE, Lotterhos KE, Crim RN, Thompson CA, Harley CDG (2011) Elevated pCO₂ increases sperm limitation and risk of polyspermy in the red sea urchin *Strongylocentrotus franciscanus*. *Glob Change Biol* 17:163–171
- ✦ Ringwood AH, Conners DE, Dinovo A (1998) The effects of copper exposures on cellular responses in oysters. *Mar Environ Res* 46:591–595
- ✦ Roesijadi G, Hansen KM, Unger ME (1996) Cadmium-induced metallothionein expression during embryonic and early larval development of the mollusc *Crassostrea virginica*. *Toxicol Appl Pharmacol* 140:356–363
- ✦ Sabine CL, Feely RA, Gruber N, Key RM and others (2004) The oceanic sink for anthropogenic CO₂. *Science* 305:367–371
- ✦ Sawatari H, Fujimori E, Haraguchi H (1995) Multi-element determination of trace elements in seawater by gallium coprecipitation and inductively coupled plasma mass spectrometry. *Anal Sci* 11:369–374
- ✦ Schäfer S, Bickmeyer U, Koehler A (2009) Measuring Ca²⁺-signalling at fertilization in the sea urchin *Psammechinus miliaris*: alterations of this Ca²⁺-signal by copper and 2,4,6-tribromophenol. *Comp Biochem Physiol C Toxicol Pharmacol* 150:261–269
- ✦ Schlegel P, Binet MT, Havenhand JN, Doyle CJ, Williamson JE (2015) Ocean acidification impacts on sperm mitochondrial membrane potential bring sperm swimming behaviour near its tipping point. *J Exp Biol* 218:1084–1090
- ✦ Schubauer-Berigan MK, Dierkes JR, Monson PD, Ankley GT (1993) pH-dependent toxicity of Cd, Cu, Ni, Pb and Zn to *Ceriodaphnia dubia*, *Pimephales promelas*, *Hyalella azteca* and *Lumbriculus variegatus*. *Environ Toxicol Chem* 12:1261–1266
- ✦ Shi W, Zhao X, Han Y, Che Z, Chai X, Liu G (2016) Ocean acidification increases cadmium accumulation in marine bivalves: a potential threat to seafood safety. *Sci Rep* 6:20197
- ✦ Shi W, Han Y, Guo C, Zhao X and others (2017) Ocean acidification hampers sperm-egg collisions, gamete fusion, and generation of Ca²⁺ oscillations of a broadcast spawning bivalve, *Tegillarca granosa*. *Mar Environ Res* 130:106–112
- ✦ Stohs SJ, Bagchi D (1995) Oxidative mechanisms in the toxicity of metal ions. *Free Radic Biol Med* 18:321–336
- ✦ Stumpp M, Dupont S, Thorndyke MC, Melzner F (2011) CO₂ induced seawater acidification impacts sea urchin larval development II: gene expression patterns in pluteus larvae. *Comp Biochem Physiol A Mol Integr Physiol* 160:320–330
- ✦ Suphamungmee W, Chansela P, Weerachayanukul W, Poomtong T, Vanichviriyakit R, Sobhon, P (2010) Ultrastructure, composition, and possible roles of the egg coats in *Haliotis asinina*. *J Shellfish Res* 29:687–697
- ✦ Thomas RC, Meech RW (1982) Hydrogen ion currents and intracellular pH in depolarized voltage-clamped snail neurones. *Nature* 299:826–828
- ✦ Thomsen J, Stapp LS, Haynert K, Schade H and others (2017) Naturally acidified habitat selects for ocean acidification-tolerant mussels. *Sci Adv* 3:e1602411
- ✦ Todgham AE, Hofmann GE (2009) Transcriptomic response of sea urchin larvae *Strongylocentrotus purpuratus* to CO₂-driven seawater acidification. *J Exp Biol* 212:2579–2594
- ✦ Ulanowicz RE, Tuttle JH (1992) The trophic consequences of oyster stock rehabilitation in Chesapeake Bay. *Estuaries* 15:298–306
- ✦ Unger ME, Roesijadi G (1996) Cd preexposure and increase in metallothionein mRNA accumulation during subsequent Cd challenge. *Aquat Toxicol* 34:185–193
- ✦ Vacquier VD, Swanson WJ, Metz EC, Stout CD (1999) Acrosomal proteins of abalone spermatozoa. *Adv Dev Biochem* 5:49–81
- ✦ Valko M, Morris H, Cronin MT (2005) Metals, toxicity and oxidative stress. *Curr Med Chem* 12:1161–1208
- ✦ Viarengo A, Pertica M, Mancinelli G, Burlando B, Canesi L, Orunesu M (1996) *In vivo* effects of copper on the calcium homeostasis mechanism of mussel gill cell plasma membranes. *Comp Biochem Physiol C Pharmacol Toxicol Endocrinol* 113:421–425
- ✦ Victor S, Richmond RH (2005) Effect of copper on fertilization success in the reef coral *Acropora surculosa*. *Mar Pollut Bull* 50:1448–1451
- ✦ Vitale AM, Monserrat JM, Castilho P, Rodriguez EM (1999) Inhibitory effects of cadmium on carbonic anhydrase activity and ionic regulation of the estuarine crab *Chasmagnathus granulata* (Decapoda, Grapsidae). *Comp Biochem Physiol C Pharmacol Toxicol Endocrinol* 122:121–129
- ✦ Wang WX, Yang Y, Guo X, He M, Guo F, Ke C (2011) Copper and zinc contamination in oysters: subcellular distribution and detoxification. *Environ Toxicol Chem* 30:1767–1774
- ✦ Wang Q, Cao R, Ning X, You L and others (2016) Effects of ocean acidification on immune responses of the Pacific oyster *Crassostrea gigas*. *Fish Shellfish Immunol* 49:24–33
- ✦ Weng N, Wang WX (2014) Variations of trace metals in two estuarine environments with contrasting pollution histories. *Sci Total Environ* 485–486:604–614
- ✦ Zhai W (2018) Exploring seasonal acidification in the Yellow Sea. *Sci China Earth Sci* 61:647–658

APPENDIX.

Table A1. Cu and Zn concentrations of test solutions used in experiments testing larval deformation and shell length in *Crassostrea angulata*

Replicate	pCO ₂ (μ atm)	Normal concentration (μ g l ⁻¹)	Tested concentration (μ g l ⁻¹)	
Cu	1	400	5	5.43
	2	400	5	5.49
	3	400	5	5.23
	4	400	5	5.80
	1	400	10	10.64
	2	400	10	10.37
	3	400	10	10.27
	4	400	10	10.36
	1	800	5	5.16
	2	800	5	5.82
	3	800	5	5.61
	4	800	5	5.83
	1	800	10	9.11
	2	800	10	10.90
	3	800	10	10.08
	4	800	10	10.78
	1	1500	5	5.12
	2	1500	5	5.23
	3	1500	5	5.16
	4	1500	5	4.73
1	1500	10	9.66	
2	1500	10	9.23	
3	1500	10	9.66	
4	1500	10	10.20	
Zn	1	400	25	28.98
	2	400	25	28.54
	3	400	25	30.01
	4	400	25	27.09
	1	400	50	51.64
	2	400	50	51.45
	3	400	50	52.07
	4	400	50	53.86
	1	800	25	26.41
	2	800	25	27.59
	3	800	25	27.69
	4	800	25	25.50
	1	800	50	53.99
	2	800	50	54.15
	3	800	50	51.33
	4	800	50	52.21
	1	1500	25	27.26
	2	1500	25	30.40
	3	1500	25	30.13
	4	1500	25	29.82
1	1500	50	55.74	
2	1500	50	54.88	
3	1500	50	57.71	
4	1500	50	52.09	